

Possible scenarios for soft and semihard component structure in central hadron-hadron collisions in the TeV region

A. Giovannini

Dipartimento di Fisica Teorica and I.N.F.N.—sezione di Torino, via P. Giuria 1, 10125 Torino, Italy

R. Ugoccioni

CENTRA and Departamento de Física (I.S.T.), Avenida Rovisco Pais, 1096 Lisboa codex, Portugal

(Received 26 October 1998; published 7 April 1999)

Three possible scenarios in hh collisions in the TeV region are discussed in full phase space in the framework of a two-component model. In the first scenario we assume that KNO scaling is achieved independently in the soft and semihard components. In the second one it is proposed that the semihard component violates heavily KNO scaling. The third scenario is a QCD inspired scenario, whose predictions turn out to be intermediate between the previous two. Recent data by E735 experiment favor strong KNO scaling violation and $\log\sqrt{s}$ increase of the average charged multiplicity of the semihard component, resulting in huge minijet production. [S0556-2821(99)04707-4]

PACS number(s): 13.85.Hd, 13.87.Fh

I. INTRODUCTION

The study of final particle multiplicity distributions (MDs) and related correlation structures in the new foreseen energy domain in the TeV region in hadron-hadron (hh) collisions is a challenging problem for multiparticle dynamics. Here the production of events with a huge number of final particles is indeed the most spectacular and fascinating although not yet fully understood phenomenon. The new fact is the occurrence of high parton density islands in regions where QCD parton evolution equations cannot be applied, and long range correlations among produced particles are expected to be quite large.

A sound theory of strong interactions cannot avoid describing such a complex high-energy many-body system; at the same time to approach this problem is ancillary to the understanding of even more complex strongly interacting systems such as proton-nucleus and heavy ions collisions. It should be recalled and stressed again and again that it is still a problem for QCD (in hh collisions more than in other collisions due to the mentioned complexity of the reaction) how to extend the theory from the perturbative to the non-perturbative sector. Hadronization mechanism and more specifically how to calculate from first QCD principles multiplicity distributions and correlation structure of final particles states (the true observables) are here unanswered questions. In this region where standard QCD has shy predictions for a complex system such as hadron-hadron scattering at very high c.m. energies one can rely only on models based on empirical observations on multiplicity distributions behavior and related normalized factorial and cumulant moments both in full phase space, and in limited sectors of rapidity and transverse variables. Thus the first step of our program is to examine critically what one learns on hh collisions in full phase space from previous experimental and theoretical work starting from accelerator region results (in a subsequent paper we will extend our study to rapidity intervals). Important hints are also expected to come from other reactions such as

e^+e^- annihilation and deep inelastic scattering, where the simplicity of the projectile and/or of the reaction itself already allowed us to isolate very interesting properties of the most elementary substructures (jets of given flavor [1,2]) at work in the interaction region.

The aim of this paper is to explore charged particle multiplicity distributions and corresponding correlation structure in hadron-hadron collisions in the TeV region in full phase space within the just sketched general phenomenological framework by using the abovementioned collective variables. Accordingly, we propose to describe MDs in full phase space in the new region in terms of the weighted superposition of the MDs of soft events (events without minijets¹) and semihard events (events with minijets), with each component assumed to be of Pascal (or negative binomial) multiplicity distribution, Pa(NB)MD,² type [3]. With these two simplifications the full problem is reduced to determine the energy dependence of the Pa(NB)MD parameters, i.e., of the average charged multiplicity \bar{n} and of parameter k for the soft and semihard components (remember that the parameter k is linked to the dispersion D by

$$k^{-1} = \frac{D^2 - \bar{n}}{\bar{n}^2}; \quad (1)$$

we also notice in passing that, when the distribution is not a Pa(NB)MD, Eq. (1) can be taken as a definition for the parameter k in terms of dispersion and average multiplicity.

It appears that in this essential framework at least three scenarios are possible: (1) Koba-Nielsen-Olesen (KNO) scal-

¹Here we rest with the standard definition of minijets as proposed by the UA1 Collaboration: groups of particles having total transverse energy larger than 5 GeV.

²From now on the abbreviation ‘‘Pa(NB)MD’’ will be used to mean the Pascal (also known as negative binomial) multiplicity distribution.

ing limit is achieved in the TeV region for both components; (2) KNO scaling is valid for the soft component, but it is heavily violated for the semihard component in the TeV region; (3) a QCD-inspired scenario can be obtained by assuming that the form of perturbative QCD predictions for the width of the MD can be used also in the nonperturbative sector.

The first two scenarios should be considered quite extreme possibilities. They determine in a certain sense reasonable bounds to the variation of the Pa(NB)MD parameters. The third one turns out to give Pa(NB)MD parameters behavior intermediate between the first two.

We are aware of the fact that the assumptions of the proposed description are not unique. They are dictated to us by our experience in the field and by our personal taste. This consideration notwithstanding we believe that this research line should be pursued in order to give some hints to future experimental and theoretical work, and to explore whether new phenomena are predicted by the present approach at higher energies. Our findings should be confronted with results of other possible phenomenological approaches (which we are demanding) leaving to experiments, when available, to decide among different realistic alternatives.

Our aim is to illustrate the Pa(NB)MD composition technique and to apply it to a simple problem. Of course, one relevant fraction of events is expected to come also from diffraction which affects both the soft and semi-hard components. Accordingly, one can study in this context substructures generated by diffraction in the two previous components by using again the composition in terms of weighted Pa(NB)MDs of diffractive and non-diffractive events. The use of a Pa(NB)MD for describing diffractive events leads indeed to results not far from those of a modified gamma distribution [4]. We do not intend to explore for the moment this new perspective, which we postpone to future work, but which we are ready to use when a correct residual analysis on MDs will show indications of new substructures. What is studied in this paper is indeed the structure of non-single-diffractive events only.

II. P_n VS n BEHAVIOR AND H_q VS q OSCILLATIONS IN FULL PHASE SPACE IN THE GEV AND IN THE TEV ENERGY DOMAINS

It has been shown in the accelerator region that final n charged multiplicity distributions in full phase space P_n are initially narrower than a Poisson distribution [$1/k$ Pa(NB)MD parameter is negative] and the distribution is indeed a binomial distribution, produced particles are very few and like to stay far apart one from the other, particles anticorrelations seem here to be favored. Then at approximately 30 GeV c.m. energy the observed MD becomes Poissonian: Pa(NB)MD parameter $1/k$ is zero in this region, particles are produced independently one from the other (as predicted by the naive multiperipheral model). Above 30 GeV c.m. energies up to ISR energies the distribution is a true Pa(NB)MD: $1/k$ parameter becomes positive, the number of produced particles is larger, two particle correlation are dominant as requested by hierarchical correlations structure. A single

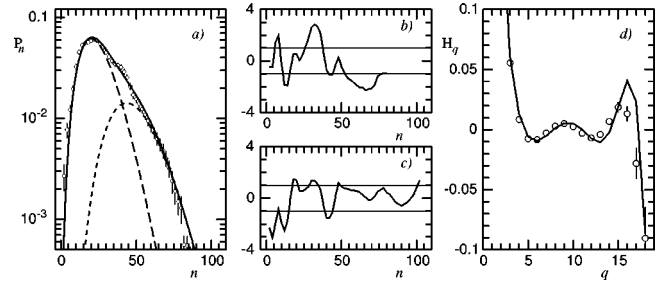


FIG. 1. (a) Multiplicity distribution at c.m. energy 546 GeV (UA5 data), with the two components of Eq. (2), corresponding residual analysis of (b) a fit with one single Pa(NB)MD and of (c) the fit with Eq. (2); (d) ratio of moments H_q , calculated from Eq. (2) after truncation.

Pa(NB)MD due to the flexibility of its $1/k$ parameter is describing quite well all the abovementioned experimental facts, which are apparently dominated by soft events. A shoulder structure in the tail starts then to appear at higher energies as shown by the UA5 Collaboration [5]; a single Pa(NB)MD cannot describe the new effect [one talks of Pascal (negative binomial) regularity violation], which can be interpreted as the onset of semihard events (events with minijets). Notice that PYTHIA Monte Carlo calculations give at present unsatisfactory results in this area [6], although a careful optimization of the parameters can of course improve this trend.

Accordingly, as reminded in the Introduction, it has been proposed to describe the observed shoulder structure as the weighted superposition of soft events (events without minijets) and semihard events (events with minijets), the weight being the fraction of soft events and the MD of each component being of Pa(NB)MD type. The resulting master equation for P_n turns out to be the following:

$$\begin{aligned}
 P_n(\alpha_{\text{soft}}; \bar{n}_{\text{soft}}, k_{\text{soft}}; \bar{n}_{\text{semihard}}, k_{\text{semihard}}) \\
 = \alpha_{\text{soft}}(\sqrt{s}) P_n^{(\text{PaNB})}[\bar{n}_{\text{soft}}(\sqrt{s}), k_{\text{soft}}(\sqrt{s})] \\
 + [1 - \alpha_{\text{soft}}(\sqrt{s})] P_n^{(\text{PaNB})}[\bar{n}_{\text{semihard}}(\sqrt{s}), k_{\text{semihard}}(\sqrt{s})]
 \end{aligned} \tag{2}$$

whose physical content is self-explanatory. Notice that we do not consider interference terms because the classification of events as soft or semihard is based on the final hadronic state, not on the underlying partonic event.

Excellent fits have been obtained for P_n [7], an example of which is shown in Fig. 1(a): the plot of residuals [(b) and (c) in the same figure] shows how the fit gets better when using two Pa(NB)MDs [although, it should be mentioned, the fit is not completely satisfactory, which can indicate the presence of further substructures. The use of residuals should also be taken *cum grano salis* in this case, because a minimum chi-square test has been used to find the Pa(NB)MDs parameters: although the run test might still be asymptotically independent of the chi-square test, which does not use

information on the sign and sequence of the deviations, its distribution is in fact not known, thus the pattern of the residual is only indicative].³

In the fits, the soft component fraction decreases from 93% at 200 GeV to 72% at 900 GeV, k_{soft} is taken constant as the energy increases (as requested by an early KNO scaling behavior) and its best fit numerical value is 7, whereas k_{semihard} decreases from 79 at 200 GeV (it describes a nearly Poissonian behavior) to 13 at 900 GeV, indicating strong KNO scaling violation. The average charged particle multiplicity is approximately two times larger for the semihard component than for the soft component (as observed by UA1 Collaboration [8]). It is interesting (and remarkable) that H_q vs q obtained by data on multiplicity distributions oscillates in this region and that the oscillations are quite well described by the K_q over F_q ratio calculated by using Eq. (2), as shown in Fig. 1(d).

That is, in summary, all we know in the GeV region on our variables behavior. Coming to the TeV region which we want to explore we will proceed by extrapolating Eq. (2) in the new energy domain. Although highly simplified our approach still requires to determine the energy dependence of Pa(NB)MD parameters \bar{n} and k for the soft and semi-hard components, as well as of soft component fraction α_{soft} , which we propose to do in the following.

A. \bar{n}_{soft} and $\bar{n}_{\text{semihard}}$ energy dependence

For \bar{n}_{soft} it is assumed that its fitted values in the multiplicity distributions in the GeV region can be extrapolated to higher energy domains, i.e.,

$$\bar{n}_{\text{soft}}(\sqrt{s}) = -5.54 + 4.72 \ln(\sqrt{s}) \quad (3)$$

(dashed line in Fig. 2), with \sqrt{s} in GeV.

Assuming UA1 analysis on minijets to be approximately valid also at higher energies one has for $\bar{n}_{\text{semihard}}$ (short-dashed line in Figure 2):

$$\bar{n}_{\text{semihard}}(\sqrt{s}) \approx 2\bar{n}_{\text{soft}}(\sqrt{s}). \quad (4a)$$

Alternatively one can postulate that $\bar{n}_{\text{semihard}}(\sqrt{s})$ is increasing more rapidly with energy and correct Eq. (4a) by adding on its right side a $\ln^2(\sqrt{s})$ term, accordingly one obtains

$$\bar{n}_{\text{semihard}}(\sqrt{s}) \approx 2\bar{n}_{\text{soft}}(\sqrt{s}) + c' \ln^2(\sqrt{s}) \quad (4b)$$

(dash-dotted line in Fig. 2). This simple correction might take into account observed deviations from Eq. (4a) behavior at 900 GeV and estimate from the fit at the same time parameter c' in Eq. (4b), which turns out to be ≈ 0.1 .

Finally \bar{n}_{total} of the resulting multiplicity distribution in agreement with the common wisdom is given by a quadratic fit (dotted line in Fig. 2):

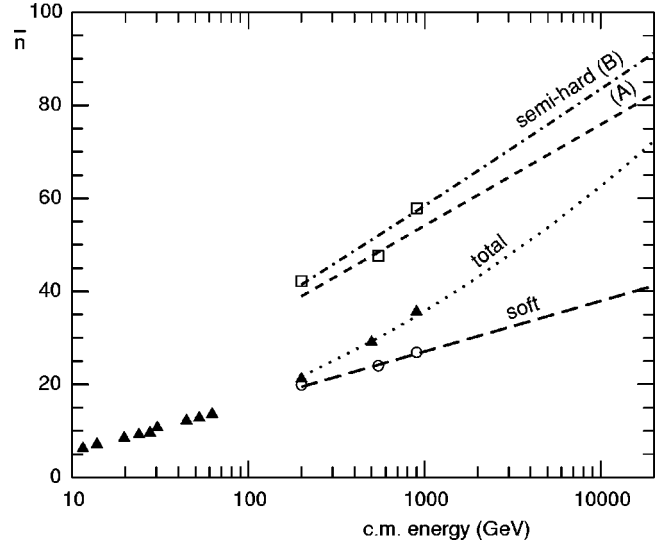


FIG. 2. Average multiplicity \bar{n} vs c.m. energy. The figure shows experimental data (filled triangles) from ISR and super proton synchrotron (SPS) colliders, the UA5 analysis with two Pa(N-B)MDs of SPS data (circles: soft component; squares: semi-hard component), together with our extrapolations [lines: dotted: total distribution; dashed: soft component; short-dashed: semi-hard component, Eq. (4a); dot-dashed: semihard component, Eq. (4b)].

$$\bar{n}_{\text{total}} = 3.01 - 0.474 \ln(\sqrt{s}) + 0.754 \ln^2(\sqrt{s}). \quad (5)$$

Being now in this approach

$$\bar{n}_{\text{total}} = \alpha_{\text{soft}} \bar{n}_{\text{soft}} + (1 - \alpha_{\text{soft}}) \bar{n}_{\text{semihard}} \quad (6)$$

the energy dependence of α_{soft} can easily be determined. It turns out to be in the two cases described by Eqs. (4a) and (4b)

$$\alpha_{\text{soft}} = 2 - \bar{n}_{\text{total}} / \bar{n}_{\text{soft}} \quad (7a)$$

and

$$\alpha_{\text{soft}} = 1 + [\bar{n}_{\text{soft}} - \bar{n}_{\text{total}}] / [\bar{n}_{\text{soft}} + c' \ln^2(\sqrt{s})], \quad (7b)$$

respectively.

In Fig. 3 the soft events fraction is shown to be quickly decreasing with energy; the general trend is to invert the situation observed in the GeV region where soft events fraction was dominant: semihard events fraction is here increasing from 11% (0.2 TeV) to 75% (20 TeV). Significant changes are introduced by the presence of the $\ln^2(\sqrt{s})$ term in Eq. (4b) at higher energies: the fraction of semihard events is in this case 10% at 0.2 TeV but increases only to 62% at 20 TeV. In the previous case, the semihard component becomes larger than the soft one at 3–4 TeV, but now the $\ln^2(\sqrt{s})$ term induces this change at approximately 7 TeV. This difference will be visible especially in scenarios 1 and 3.

³We thank S. Krasznovszky for discussion on this point.

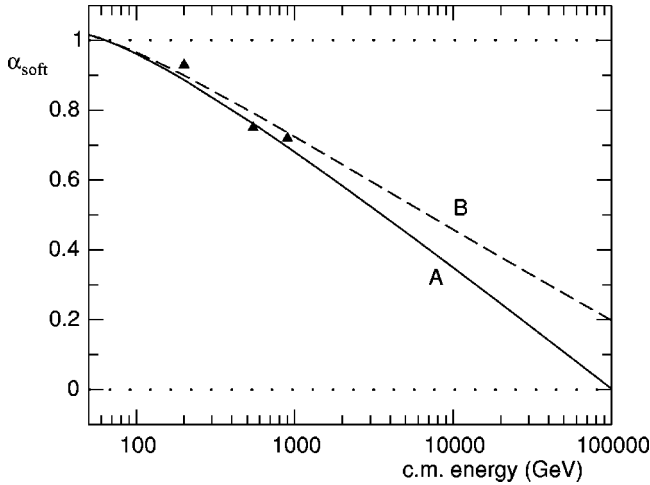


FIG. 3. Energy dependence of the superposition parameter α_{soft} (fraction of soft events) in the two cases of a linear [solid line, Eq. (4a)] and quadratic [dashed line, Eq. (4b)] dependence of the average multiplicity of the semi-hard component on c.m. energy. The triangles are the result of the UA5 analysis [7].

B. k_{soft} and k_{semihard} energy dependence

k_{soft} was found to be constant in the GeV region by the UA5 collaboration; since in addition \bar{n}_{soft} is growing with energy, see Eq. (3), to assume k_{soft} constant in the new energy domain implies

$$D_{\text{soft}}^2 / \bar{n}_{\text{soft}}^2 \approx \text{const} \approx 0.143 \quad (8)$$

which corresponds to say that KNO scaling behavior is valid for the soft component in the TeV region. We stay with this assumption on k_{soft} . It should be pointed out that k_{soft} is not affected by the introduction of the $\ln^2 \sqrt{s}$ term in Eq. (4b). As anticipated in the Introduction, the discussion on the behavior of k_{semihard} opens at least three possible scenarios which are discussed in the following.

III. THE THREE SCENARIOS

A. Scenario 1

KNO scaling holds in the TeV region also for the semi-hard component, i.e., we assume that k_{semihard} is decreasing until 900 GeV (its value is 13 at this c.m. energy) and then it remains constant in the new region. Being that $\bar{n}_{\text{semihard}}$ is even larger than \bar{n}_{soft} , $D_{\text{semihard}}^2 / \bar{n}_{\text{semihard}}^2 \approx 0.09$ throughout all the explored energy range, see Figs. 4(a) and 4(b).

The effect of a quadratic growth of $\bar{n}_{\text{semihard}}$ with energy, Eq. (4b), in this scenario is to increase the value of $1/k_{\text{total}}$ [curves B in Figs. 4(a),4(b)], via the change in α_{soft} , Eq. (7b). This fact is consistent with our assumption of the superposition mechanism.

Expected multiplicity distributions at 1.8 and 14 TeV c.m. energies and corresponding H_q vs. q oscillations fitted by using the composition of the soft and semihard substructures are shown in Fig. 5. The energies of 1.8 and 14 TeV have been chosen because they are respectively the c.m. energy of

Fermilab TEVATRON and the expected c.m. energy of the CERN Large Hadron Collider (LHC). It is interesting to remark that the shapes of the multiplicity distributions of the two components are similar at all energies, but the heights of the corresponding maxima are reversed in going from the lowest to the top energy. In addition oscillations seem to be stretched in shape as the energy increases, indicating their tendency to be highly reduced at higher energies [notice that we show here H_q moments calculated without truncating the MD, because the truncation depends solely on the size of the experimental sample; thus we only show the moments computed for the total MD, as the two components are each of Pa(NB)MD type and therefore, individually considered, show no oscillations].

A rather large change in the shape of the MD is introduced when we consider the quadratic term for $\bar{n}_{\text{semihard}}$, Eq. (4b): even at 20 TeV the maximum of the semihard component has not yet become larger than that of the soft component. On the other hand, the shoulder has become more evident, due to the higher average multiplicity that was introduced for the semihard component and the smaller resulting value of α_{soft} ; at a c.m. energy of 14 TeV the area of the maximum of the total MD is rather flat and shows a small dip [see Fig. 5(a)]. Correspondingly the oscillations of the H_q moments become approximately four times larger in amplitude, but do not vary much in period, and the first minimum is not shifted.

B. Scenario 2

The main assumption is that the general trend observed in the GeV region for the total distribution continues to be valid in the TeV region, i.e., $D_{\text{total}}^2 / \bar{n}_{\text{total}}^2$ is logarithmically growing, suggesting strong KNO scaling behavior violation:

$$k_{\text{total}}^{-1} = -0.082 + 0.0512 \ln \sqrt{s}, \quad (9)$$

see Figs. 4(c),4(d).

The effect of a quadratic growth of $\bar{n}_{\text{semihard}}$, Eq. (4b), in this scenario is to decrease the value of $1/k_{\text{semihard}}$ (curves labeled B in the figure). This fact is again consistent with $1/k_{\text{total}}$ growing with energy. In Fig. 6 are shown the multiplicity distributions and the corresponding H_q vs q oscillations of this scenario.

The first remark is that the shapes of the two components are totally different, a wide queue in the semihard component is visible in the high multiplicity channels. The heights at the maxima favor initially the soft component and then the heights of the two components are almost equal. It is striking that H_q vs q oscillations disappear as the c.m. energy increases, indicating that single Pa(NB)MD behavior is the dominant feature in this energy domain.

In this case the effect of a quadratic growth of $\bar{n}_{\text{semihard}}$ is much less noticeable than in scenario 1 in the shape of the MD: the shoulder is only slightly more visible and the amplitude of the H_q oscillations is moderately larger than in the case of linear $\bar{n}_{\text{semihard}}$.

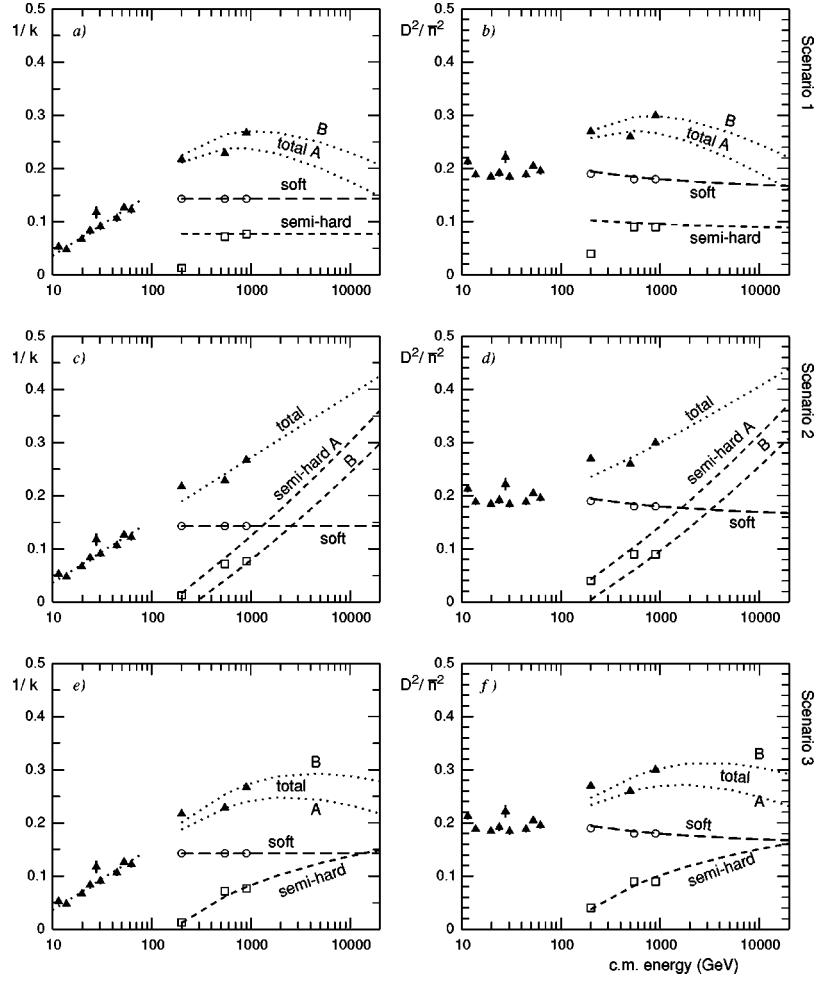


FIG. 4. The parameter $1/k$ [(a),(c),(e)] and the KNO scaling parameter D^2/\bar{n}^2 [(b),(d),(f)] are plotted for the scenarios described in the text [from top to bottom: (a),(b): scenario 1; (c),(d): scenario 2; (e),(f): scenario 3]. The figures shows experimental data (filled triangles) from ISR and SPS colliders, the UA5 analysis with two Pa(NB)MDs of SPS data (circles: soft component; squares: semi-hard component), together with our extrapolations (lines: dotted: total distribution; dashed: soft component; short-dashed: semi-hard component).

C. Scenario 3

This is the QCD inspired scenario. QCD predicts, at the leading order,⁴ for the parameter k of the multiplicity distribution [10]

$$k^{-1} = a + b\sqrt{\alpha_{\text{strong}}}, \quad (10)$$

where

$$\alpha_{\text{strong}} \approx 1/\ln(Q/Q_0) \quad (11)$$

and Q , Q_0 are the initial virtuality and the cutoff of the parton shower. QCD predicts (for e^+e^- annihilation) $a \approx 0.33$ and $b \approx -0.9$, but in order to apply the above equation to our problem we leave the a , b , and Q_0 parameters free.

⁴In view of the approximations involved, more sophisticated calculations [9] are not useful in this framework.

Since the constants can be determined by a least square fit to the values found for k at c.m. energies 200, 500, and 900 GeV one obtains, assuming Eq. (10) to control $k_{\text{semi-hard}}$ component behavior,

$$k_{\text{semi-hard}}^{-1} = 0.38 - 0.42/\sqrt{\ln(\sqrt{s}/10)}. \quad (12)$$

The result is presented in Figs. 4(e),4(f). Notice how $1/k_{\text{total}}$ is indeed lower than in scenario 2 but higher than in scenario 1. The effect of a quadratic growth of $\bar{n}_{\text{semi-hard}}$, Eq. (4b), in this scenario is once again to increase the value of $1/k_{\text{total}}$ similarly to what happens in scenario 1.

The new situation for P_n vs n and H_q vs q is summarized in Fig. 7. It is interesting to remark that this scenario gives predictions on both variables which are intermediate between the two previous extreme ones of scenarios 1 and 2. In Fig. 7(a) one sees in fact that the tail of P_n vs n is increasing with c.m. energy but high multiplicity channels are not populated as in Fig. 6, although they are larger than those in Fig. 5. Minijets production is intermediate between the two scenarios. Accordingly, in Fig. 7(b) H_q vs q oscillations are

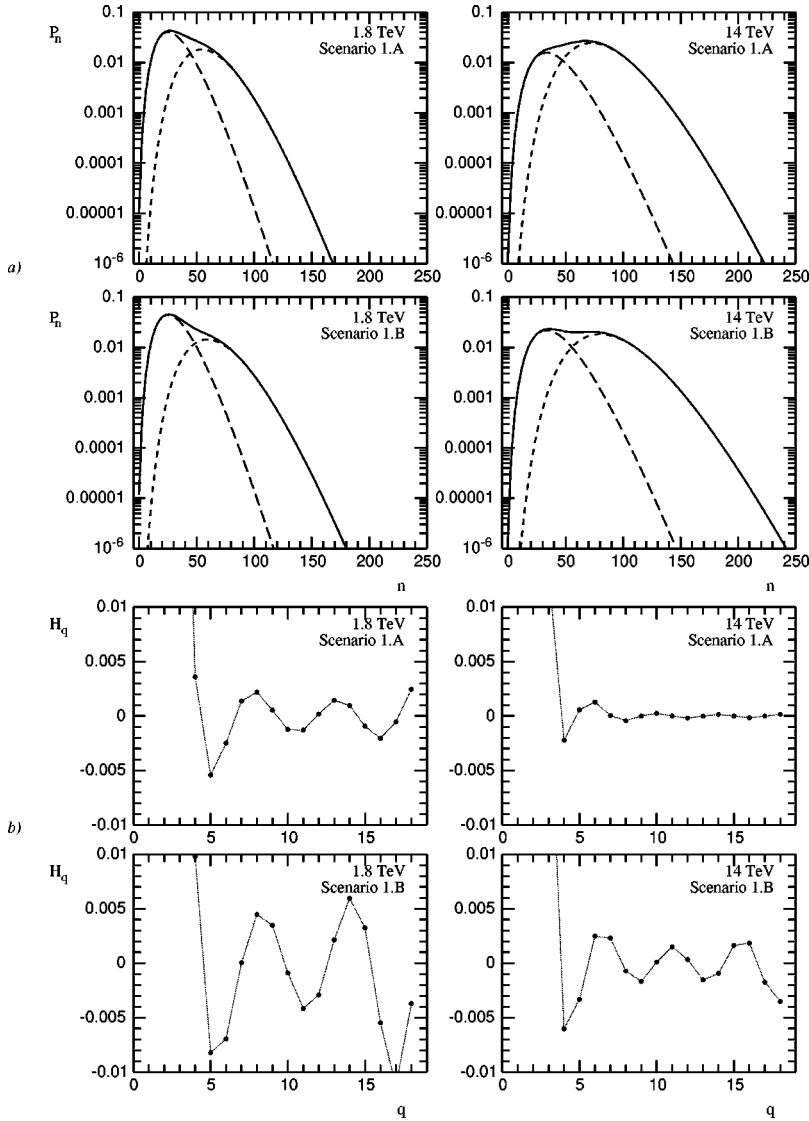


FIG. 5. (a) Multiplicity distributions for scenario 1 at c.m. energies of 1.8 (Tevatron energy) and 14 (LHC expected energy) TeV; the first row refers to solution A for the average multiplicity in semihard events, the second row to solution B (solid line: total distribution; dashed line: soft component; short-dashed line: semihard component). (b) filled circles: H_q vs q oscillations (without truncation of the MD) corresponding to the total distribution of part (a); the line is drawn to guide the eye; again the first row refers to solution A for the average multiplicity in semi-hard events, the second row to solution B.

decreasing with c.m. energies but not as much as in scenario 2, indicating that the absence of oscillations is here an asymptotic prediction and coincides with expectations of H_q oscillations description in terms of a single Pa(NB)MD. It is in fact quite clear that in the limit $\alpha_{\text{soft}} \rightarrow 0$ minijets production is dominant with respect to soft events and the corresponding multiplicity distribution is described almost fully by a single Pa(NB)MD.

The effect of a quadratic growth of $\bar{n}_{\text{semihard}}$ is quite noticeable here, as the shoulder structure, almost disappeared above 10 TeV with linear $\bar{n}_{\text{semihard}}$ is now well visible up to 20 TeV, because the semihard component has not yet become dominant. Correspondingly, H_q oscillations are approximately 3 times as large as in the linear case.

It appears that probably it is a too ‘‘black and white’’ attitude to assume for k_{semihard} strong KNO scaling behavior

(scenario 1) or strong KNO scaling violation (scenario 2). These too extreme choices were done of course on purpose in order to fix the boundary conditions to our exploration: the real world might very well be (as illustrated by scenario 3) between the above two.

In conclusion the reaction is controlled by the ratio of soft to semi-hard events. This ratio favors soft events production up to CERN Intersecting Storage Rings (ISR) energies and a single Pa(NB)MD describes here quite well all experimental facts, above such energies semihard events start to play a more important role and are revealed by two effects (the onset of shoulder structure in the multiplicity distributions and H_q vs q oscillations in related correlations); both effects can be cured by using the weighted composition of two Pa(NB)MDs, one for the soft part of the reaction, and the second for its semihard part. In the TeV region semihard

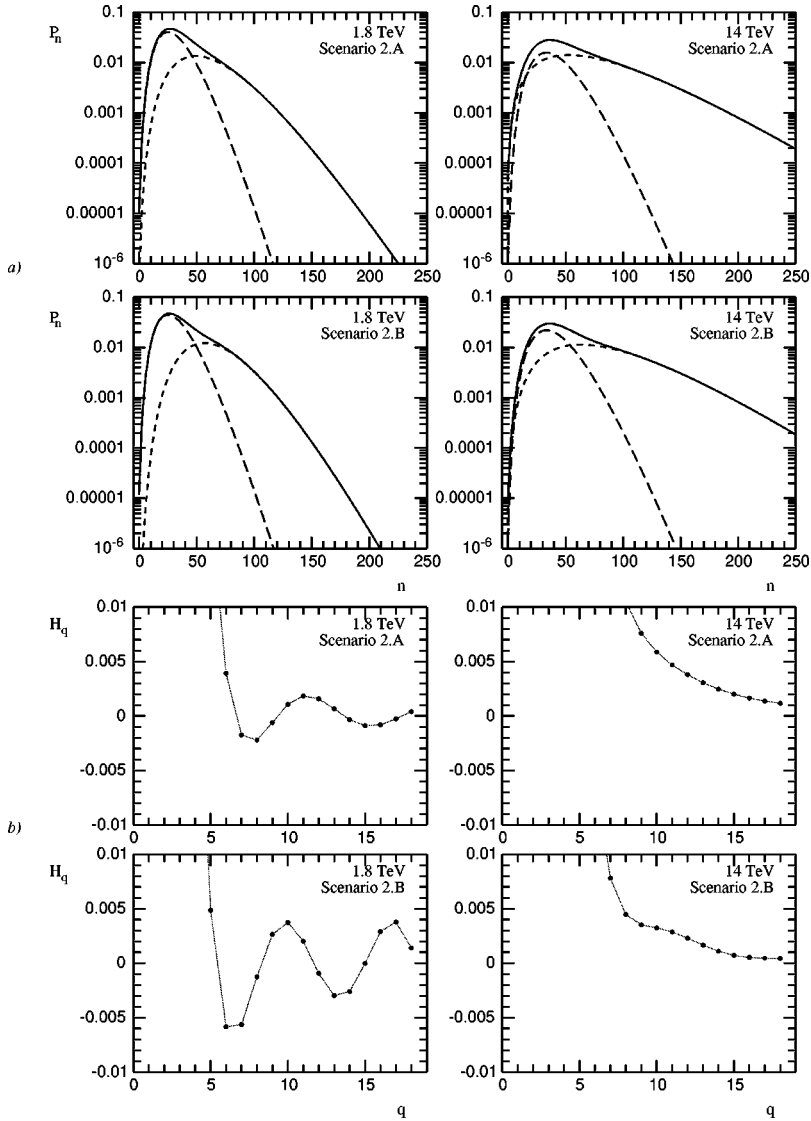


FIG. 6. Same content as Fig. 5 but for scenario 2.

events become dominant, they obscure soft events production and following our assumptions asymptotically ($\alpha_{\text{soft}} \rightarrow 0$) a single Pa(NB)MD is describing again quite well multiplicity distributions and corresponding correlation structure. A quite natural question after these remarks is how soft and semihard events, being both described in terms of a Pa(NB) multiplicity distribution, can be distinguished in the framework of clan structure analysis.

IV. CLAN ANALYSIS OF THE SOFT AND SEMIHARD COMPONENT SUBSTRUCTURES

For a single Pa(NB) MD of standard \bar{n} and k parameters, clan structure analysis [11,12] is performed in terms of the average number of clans \bar{N} and of the average number of particle per clan \bar{n}_c which are defined as follows:

$$\bar{N} = k \ln(1 + \bar{n}/k), \quad \bar{n}_c = \bar{n}/\bar{N}, \quad (13)$$

see Fig. 8. The above definition is valid for a single Pa(NB)MD only. Notice that for the total multiplicity distribution, clans cannot be defined: the fact, as shown in Figs. 5–7, that the total MD presents oscillations in the ratio of moments H_q implies, via the theorems proven in Ref. [13], that the total MD is not an infinitely divisible distribution (IDD): indeed only for IDDs it is possible to generalize the definition of clans from that of Eq. (13) to that of intermediate sources produced according to a Poisson distribution. This is the reason why we will discuss the behavior of clan parameters only for each component separately.

The soft component substructure is the same in all three scenarios. The average number of clans is here a slowly increasing variable with c.m. energy and the average number of particles per clan goes from 2.6 at 1.8 TeV to 3.1 at 20 TeV, indicating that phase space is homogeneously filled by independent almost equal size clans as requested by a KNO scaling regime. One can talk in this context pictorially of independent equally populated sources whose number is a slowly increasing function of available c.m. energy.

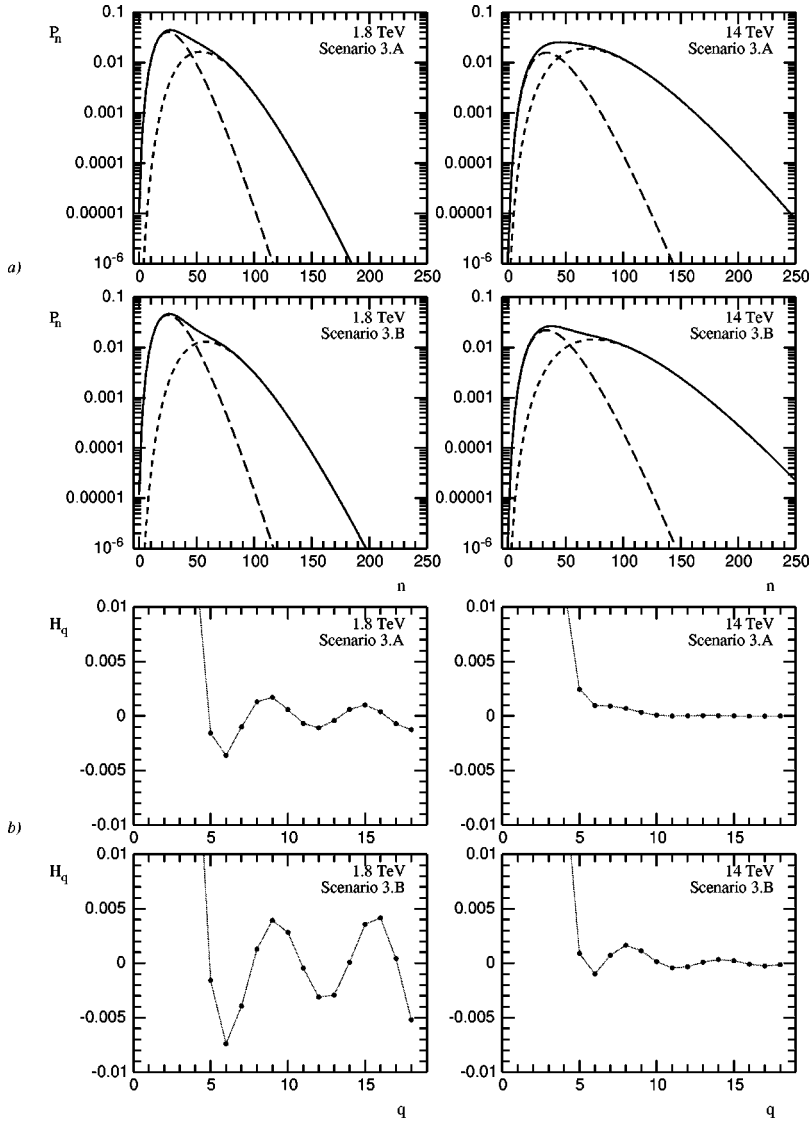


FIG. 7. Same content as Fig. 5 but for scenario 3.

In scenario 1, which assumes KNO scaling behavior also for the semihard component, the average number of particles per clan is approximately the same as that seen in the soft component substructure, whereas the average number of clans is two times larger in the semihard component than in the soft one. This finding is consistent with the assumption of equation (4a). It is quite difficult in this scenario to see any sizeable difference between soft and semihard clans. Apparently clans have indeed the same size in both classes of events; the difference lies only in the average number of clans which is two times larger in the semihard component.

Scenario 2 shows a dramatic increasing with energy of the $D_{\text{semihard}}^2/\bar{n}_{\text{semihard}}^2$ ratio as requested by strong KNO scaling violation. Accordingly the average number of clans is a quickly decreasing function of energy and then it becomes a very slowly decreasing quantity. This behavior should be confronted with that of the average number of particles per clan which at 5 TeV is almost two times larger than at 900 GeV and becomes three times larger at 20 TeV. Notice that this huge cascading phenomenon is associated with a limited

number of independent intermediate sources and this is striking. The two scenarios are indeed—as already mentioned—quite extreme. The highly ordered and homogeneous structure of phase space in scenario 1 becomes here highly inhomogeneous favoring huge branching production in each source to be compared with the fully independent production of the sources (clans). Available c.m. energy goes more in particle production within a clan than in clan production, contrary to what was found in scenario 1. Here equal size, more numerous soft clan production in soft events, should be contrasted with less numerous semi-hard clans of quickly growing size in semihard events. One can guess that it is the high internal branching within each semihard clan which is responsible of the huge minijet production and favors even clustering of minijets.

Finally scenario 3 which, it should be remembered, is a QCD inspired scenario. KNO scaling violation for the semihard component although effective is not as strong as in scenario 2. The average number of clans is 18.2 at 5 TeV (about the same size seen at 900 GeV) and 17.5 at 20 TeV,

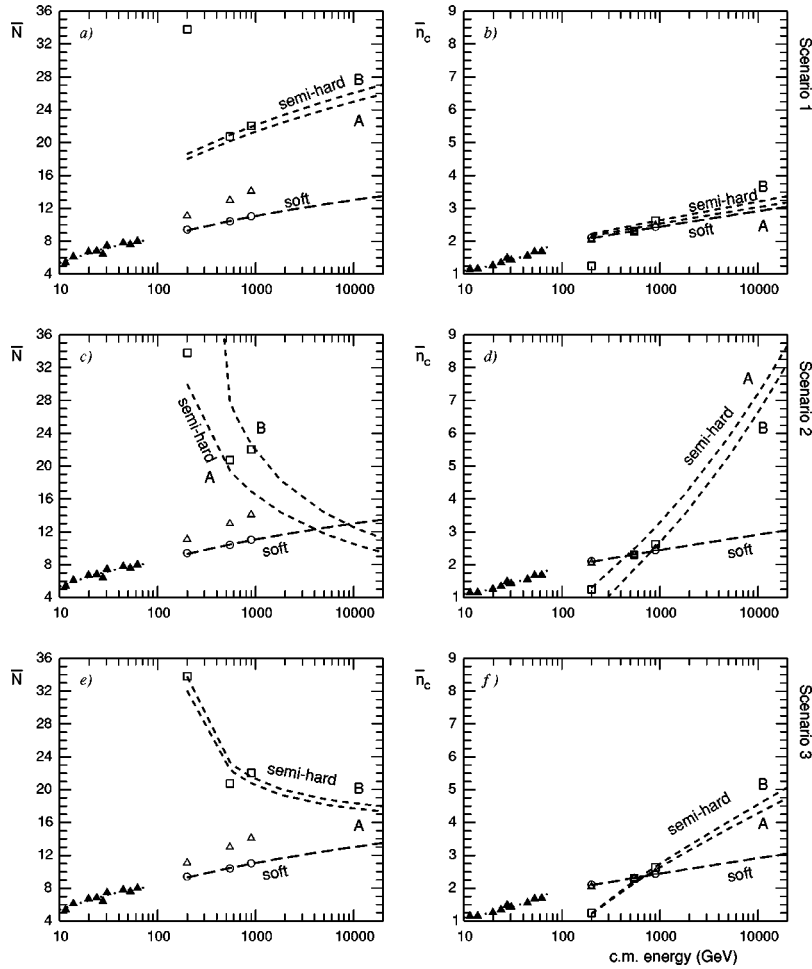


FIG. 8. Clan parameters \bar{N} [(a),(c),(e)] and \bar{n}_c [(b),(d),(f)] are plotted for the scenarios described in the text [from top to bottom: (a),(b): scenario 1; (c),(d): scenario 2; (e),(f): scenario 3]. The figures shows experimental data (filled triangles) from ISR and SPS colliders, the UA5 analysis with two Pa(NB)MDs of SPS data (circles: soft component; squares: semihard component), together with our extrapolations (lines: dotted: total distribution; dashed: soft component; short-dashed: semihard component).

suggesting an almost energy independent production of the average number of clans over a large fraction of the TeV region; in addition the average number of particles per clan is growing with energy but not as much as in scenario 2, suggesting a moderate average branching consistent with particle production in minijets.

In Fig. 8 \bar{N} and \bar{n}_c are plotted for the individual substructures of the collision in the three scenarios as functions of the c.m. energy. It is interesting to remark here on a linear growth of \bar{N} with the maximum allowed rapidity for the soft component and for the semihard component of scenario 1 to be contrasted with an almost parabolic decrease of the average number of clans for the semihard component in scenarios 2 and 3 with respect to the same variable. It is also remarkable that the average number of clans is more rapidly decreasing in scenario 2 than in scenario 3, indicating the occurrence of more branching in each clan. In addition in scenario 3 the starting of a very slowly decreasing region for \bar{N} is already clearly visible at 10 TeV and expected to develop over a large sector of the TeV region.

The effect of a quadratic growth of $\bar{n}_{\text{semihard}}$, Eq. (4b), is

visible only in scenario 2, being negligible in scenarios 1 and 3; obviously the effect appears only in the semihard component, and not in the soft one. These facts are a consequence of how we constructed our scenarios: indeed in scenarios 1 and 3 the term $\ln^2(\sqrt{s})$ appears only in \bar{n} inside the logarithm [see Eq. (13)], whereas in scenario 2 it appears also in k_{semihard} . The average number of clans is increased by about 20%, while the average number of particles per clan is decreased by approximately 10%.

V. NEW EXPERIMENTAL DATA

After we finished our work, the paper by Matinyan and Walker [14] appeared, providing data from the E735 experiment at FERMLAB. The Authors of that paper find that MD data in f.p.s. up to 1800 GeV c.m. energy can be described in terms of events belonging to two independent classes, only one of which obeys KNO scaling. The threshold for the appearance of the second class of events is estimated approximately between 100 and 200 GeV. These results agree with the starting point of the present analysis. The authors of Ref.

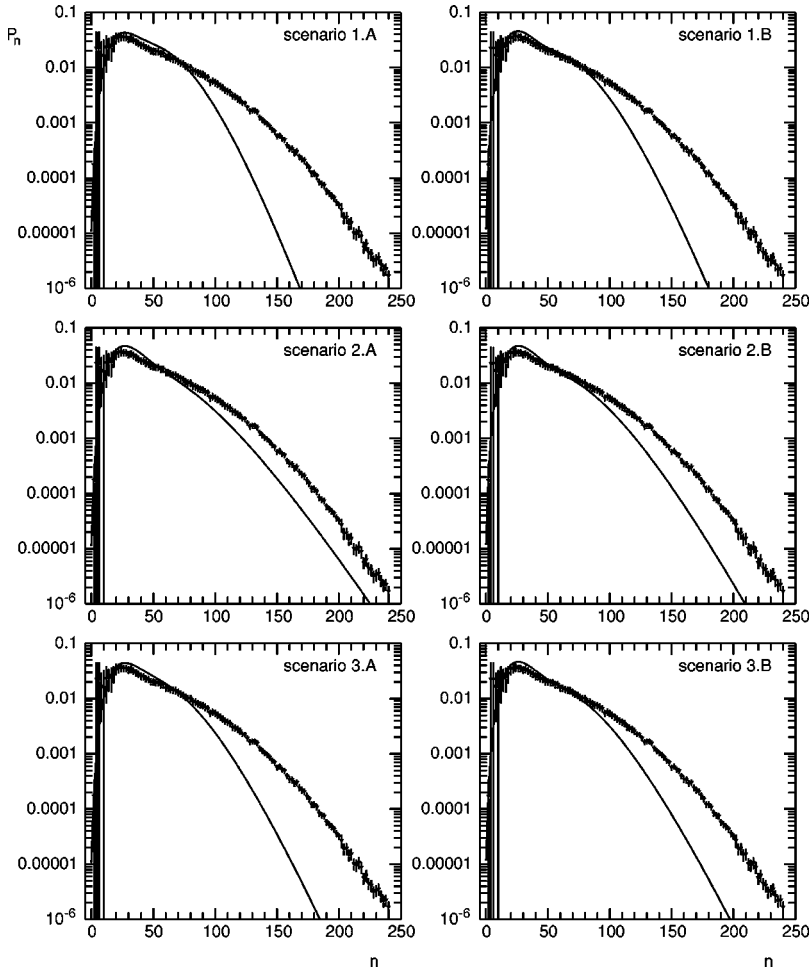


FIG. 9. Comparison of our predictions on MDs at 1.8 TeV c.m. energy (solid lines) with the recent data published by the E735 Collaboration (triangles) [14] for each scenario and each option.

[14] interpret the two classes as events generated by one and by more than one parton-parton collision, respectively. Alternatively, we prefer to interpret the two classes as soft and semihard events. It should be remarked that in the data presented by the E735 experiment the MD are systematically wider than the corresponding ones of the UA5 Collaboration. This consideration notwithstanding, we decided to compare the new data at 1.8 TeV c.m. energy to our predictions, presented in the previous sections. As can be seen in Fig. 9, just by inspection, scenario 2 with option A seems to be favored.⁵ We conclude that according to our description one should expect strong KNO scaling violation in the MD and logarithmic growth with energy of the average charged multiplicity of the semihard component. It is interesting to remark that what we considered an extreme situation turns out to be less extreme from an experimental point of view: it is clear indeed that a huge minijet production will be the main characteristic of the new energy domain. Assuming that observed deviations of E735 results from our predictions of scenario 2

in Fig. 9 will be confirmed, they imply that our k_{semihard} parameter decreases more rapidly than in our scenario. This fact has important consequences since the mentioned deviations occur mainly in the tail region of the distribution, where the multiplicity is higher. Accordingly, the integrated two-particle correlation, $\int C_{2,\text{semihard}}(\eta_1, \eta_2) d\eta_1 d\eta_2 = \bar{n}_{\text{semihard}}^2 / k_{\text{semihard}}$, are much larger. Therefore one should expect here a production of more densely populated minijets characterized by a higher internal two-particle correlation structure. This fact can be best understood in terms of clan structure analysis: as discussed in Sec. IV, clans are few and very large under the conditions just described, indicating that very productive branching processes are at work.

Whether this is the onset of a new component to be added to the previous ones and to be interpreted as the corresponding phenomenon to the occurrence of three independent and simultaneous parton-parton collisions as implicitly suggested by the authors of Ref. [14], or simply a discrepancy which should be cured by modifying the energy dependence of Pa(NB)MD parameters in our scenarios (and especially in scenario 2 with option A) is an open question. A clarification can come by a comparison of E735 results with CDF data and a better understanding of the phenomenon itself by the

⁵A more detailed discussion on the experimental results of the E735 Collaboration and their relevance for the study of MDs in the TeV region is postponed to a forthcoming paper.

analysis of data at TEVATRON in rapidity intervals which probably are affected by less systematic errors than in full phase space. Accordingly, we prefer to be more cautious and to wait for new data before drawing any ultimate conclusion.

VI. SUMMARY

Possible scenarios of multiparticle production in hadron-hadron collisions in the TeV region have been discussed. It has been shown that the most spectacular facts are here the occurrence of two classes of events and in this framework the dominance of semihard events with respect to the soft ones; this last result should be confronted with the behavior of the two components in the GeV region where just the opposite occurs, i.e., the soft component is dominant. Assuming that soft component events multiplicity distributions behave according to KNO scaling expectations, two extreme situations for the semihard component structure of the multiplicity distributions, i.e., an effective KNO scaling regime and a strong KNO scaling violation regime, have been compared to a QCD inspired set of predictions. Essential ingredient of the analysis have been to think to the final charged particle multiplicity distributions at various energies in terms of the weighted superposition of the two abovementioned components, the weight being the fraction of soft events. In addition following the success of the fits in the GeV region each component has been assumed to be of Pa(NB)MD type.

Scenario 1 is apparently excluded by E735 data at 1.8 TeV c.m. energy and scenario 2, when compared with the same set of data, turns out to be less extreme than previously thought suggesting that the main feature in the new region, in our framework, is huge minijet production together with a possible production of a new species of minijets. The QCD inspired scenario interestingly gives predictions which are intermediate between the other two.

Clan structure analysis when applied to the identified substructures of the reaction in full phase space in the TeV region reveals unexpected and interesting properties which clearly differentiate the three scenarios and offer strong support to mentioned interpretation of scenario 2 in terms of minijets. Finally, we would like to stress once more the importance of the awaited data in rapidity intervals from TEVATRON, which, not suffering from the systematic limitations of extrapolations to full phase space (as done by UA5 and by E735) will help clarify the situation while waiting for the LHC.

ACKNOWLEDGMENTS

Both authors would like to thank W. D. Walker for useful discussions on his work. R. U. gratefully acknowledges the financial support of the Fundação Ciência e Tecnologia via the “Sub-Programa Ciência e Tecnologia do 2^o Quadro Comunitário de Apoio.”

-
- [1] A. Giovannini, S. Lupia, and R. Ugoccioni, *Phys. Lett. B* **388**, 639 (1996).
- [2] A. Giovannini, S. Lupia, and R. Ugoccioni, *Phys. Lett. B* **374**, 231 (1996).
- [3] A. Giovannini and R. Ugoccioni, *Nucl. Phys. B (Proc. Suppl.)* **64**, 68 (1998).
- [4] K. Goulianos, *Phys. Lett. B* **193**, 151 (1987); K. Goulianos, *Phys. Rep.* **101**, 169 (1983).
- [5] UA5 Collaboration, R. E. Ansorge *et al.*, *Z. Phys. C* **43**, 357 (1989).
- [6] A. Giovannini and R. Ugoccioni, in *Proceedings of the 27th International Symposium on Multiparticle Dynamics*, Frascati, Italy, 1997, edited by G. Capon, V. A. Khoze, G. Pancheri, and A. Sansoni [*Nucl. Phys. B (Proc. Suppl.)* **71**, 201 (1999)].
- [7] C. Fuglesang, in *Multiparticle Dynamics: Festschrift for Léon Van Hove*, La Thuile, Italy, 1989, edited by A. Giovannini and W. Kittel (World Scientific, Singapore, 1990), p. 193.
- [8] UA1 Collaboration, G. Ciapetti, in *Proceedings of the 5th Topical Workshop on Proton-Antiproton Collider Physics*, Saint-Vincent, Italy, 1985, edited by M. Greco (World Scientific, Singapore, 1986), p. 488.
- [9] Yu. L. Dokshitzer, *Phys. Lett. B* **305**, 295 (1993).
- [10] Z. Kunszt and P. Nason, in *Z Physics at LEP 1*, edited by G. Altarelli, R. Kleiss, and C. Verzegnassi (CERN Yellow Report No. 89-08, Geneva, 1998), Vol. 1, p. 373.
- [11] A. Giovannini and L. Van Hove, *Z. Phys. C* **30**, 391 (1986).
- [12] A. Giovannini, in *Proceedings of the XXVI International Symposium on Multiparticle Dynamics*, Faro, Portugal, 1996, edited by J. Dias de Deus *et al.* (World Scientific, Singapore, 1997), p. 232.
- [13] R. Ugoccioni, A. Giovannini, and S. Lupia, *Phys. Lett. B* **342**, 387 (1995).
- [14] S. G. Matinyan and W. D. Walker, *Phys. Rev. D* **59**, 034022 (1999); W. D. Walker, talk presented at the XXVIII International Symposium on Multiparticle Dynamics, Delphi, Greece, 1998 (unpublished); T. Alexopoulos *et al.*, *Phys. Lett. B* **435**, 453 (1998).